

# STOCHASTIC MODELING AND SIMULATION OF FIBER EVOLUTION DURING MELT-BLOWING SLAG FIBERIZATION

Dimitrios I. Gerogiorgis, Dimitrios Panias, Ioannis Paspaliaris

Laboratory of Metallurgy, School of Mineral and Metallurgical Engineering  
National Technical University of Athens (NTUA)  
9, Heroon Polytechniou Street, Zografou Campus; Athens, GR-15780, Greece

Keywords: Stochastic modeling, mineral wool, slag, fiberization, particle size distribution (PSD)

## Abstract

Red mud fiberization is a process with remarkable potential, alleviating environmental pressure by transforming an aluminum by-product into mineral wool, thus to various marketable products. A promising mineral wool process is molten slag fiberization via an impinging air jet, which avoids mechanical wear and rotating parts. A high-temperature molten slag stream is subjected to high shear, intensive droplet generation and subsequent fiber elongation: nascent mineral fibers follow independent trajectories towards a collection chamber, often breaking up to form shots (off-spec product) which either fall away from or are embedded into the mineral wool product. Fiber and shot size distributions are pivotal as a means of ensuring mineral wool product quality.

This paper focuses on stochastic modeling and simulation of molten slag fiber generation and evolution: the model encompasses published, validated correlations of dimensionless numbers within the well-defined cone of fiber dispersion. Fiber elongation and breakup along trajectories are explicitly studied, considering temperature-dependent slag transport properties and explicit variability of flight trajectory and operating conditions, towards achieving process optimization.

## Introduction

Primary aluminium is produced from bauxite ore that which is converted into aluminium oxide, which is subsequently reduced to primary aluminium by means of electrolysis (Frank, 2005). Common industrial aluminium production practice and plants consist of two (2) distinct stages: (i) the *production of metallurgical alumina* ( $\text{Al}_2\text{O}_3$ ) from bauxite, conducted according to the Bayer process and (ii) the *electrolytic reduction of alumina to aluminium*, which is performed according to the Hall-Héroult process; both processes have been developed in the 19<sup>th</sup> century. Although both have been extensively investigated and optimized via technological breakthroughs (Haupin, 2001), their scientific principles and environmental issues have remained unchanged. Alternative processes, such as carbothermic aluminium production, have been the focus of long and sustained industrial interest; production-scale progress has been recently achieved via many experimental campaigns and concurrent mathematical and CFD modeling (Gerogiorgis, 2004).

In order to improve significantly the Bayer process energy and exergy efficiency and reduce substantially its environmental footprint, an arsenal of innovative technologies is required so as to transform red mud into marketable products of sustainable industrial interest (Wang, 2008). Red mud is a visible, inevitable Bayer process by-product with environmental impact, containing heavy metals (Santona, 2006) and oxides (Maitra, 1994) which worth recovering (Kumar, 2006). The proposed process (Balomenos, 2010) uses a novel Electric Arc Furnace (EAF) technology (AMRT, 2011) to achieve the reductive smelting of red mud without laborious pre-treatment, thus producing pig iron of required purity and viscous slag suitable for mineral wool production.

This novel EAF is the Advanced Mineral Recovery Technology (AMRT) melt reduction furnace, capable of processing finely sized materials without any loss of dusty material in off-gas streams. An innovative feeder delivers the dusty raw materials directly into the electric arc zone, and a digital PLC control system minimizes electric energy losses by continuous measurement of power supply and bath impedance (AMRT, 2011). This EAF innovation is ideal for processing dust-like red mud produced by aluminium plants (mean particle size is less than 500 nm) without any pre-treatment and without substantial energy losses, providing a crucial industrial advantage.

The novel red mud treatment process which has been proposed under the auspices of ENEXAL comprises three distinct stages: feedstock preparation, reductive smelting and product handling. In the *feedstock preparation stage* (Stage 1) the bauxite residue is first processed in a dryer (using the countercurrent heat of the furnace off-gases) to remove the water left in the residue. The dry bauxite residue is moved to the material weighing and mixing unit, where it is blended with fluxes (CaO, SiO<sub>2</sub>) to regulate its transport properties, and coke (C) fines towards reduction. In the *reductive smelting stage* (Stage 2), the mixture is fed automatically via the electronically controlled AMRT Furnace Feeding Unit to the bowl of the AMRT Furnace, where a melt of 1590 °C-1610 °C is sustained throughout the reductive smelting process (3-5 hours per batch). All off-gases generated in the AMRT Furnace (as soon as they have passed through the dryer) are filtered in an adjacent baghouse and subsequently discharged (purified) to the atmosphere. Upon completion, two immiscible liquid phases (molten slag and pig iron) remain in the furnace. In the *product handling stage* (Stage 3), the two phases are separated via sequential decantation (by tilting the furnace bowl on its horizontal axis), due to a considerably high density difference. The lighter slag phase is channeled into a fiberization unit and finely dispersed to mineral wool, motivating a multiscale technical problem which forms the exclusive focus of the present paper. The heavier metal phase is poured into refractory moulds and solidifies, producing pig-iron slabs.

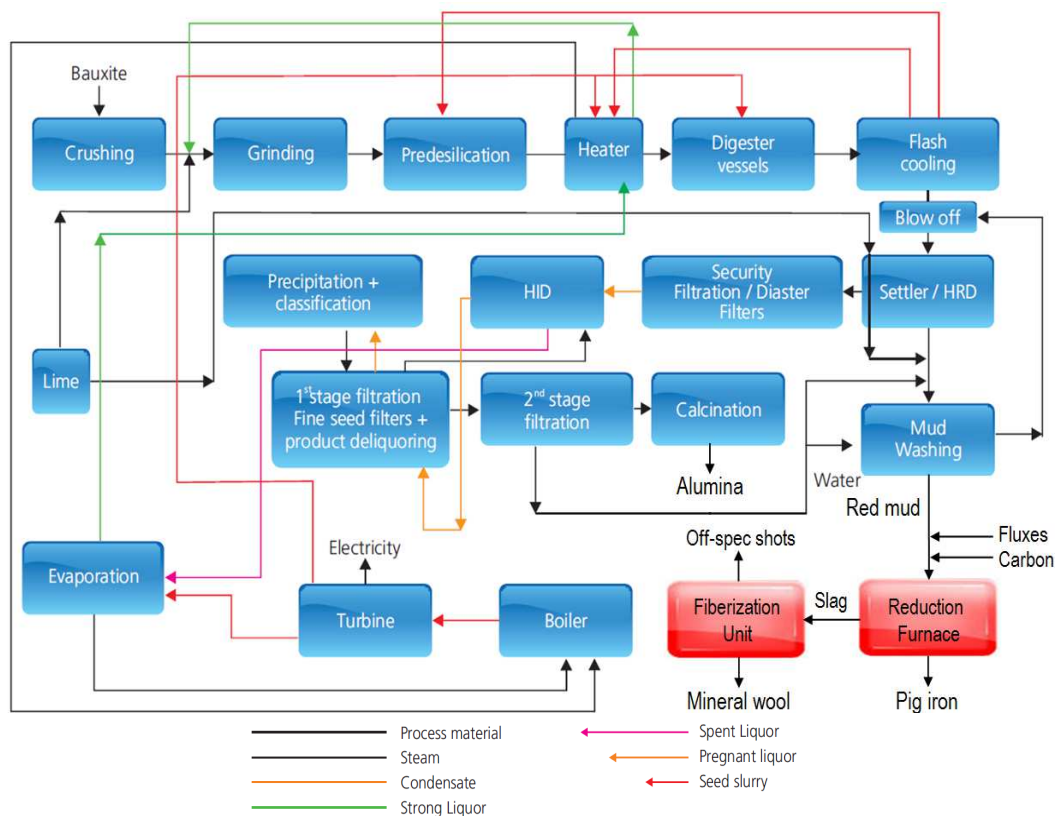


**Figure 1.** Process block diagram towards sustainable molten slag fiberization of red mud after alumina production.

## Fiberization and Mathematical Modeling Strategy

A schematic presentation of the fiberization process via impinging gas jet is presented in Fig. 2a. The molten slag flows over a system of adjustable channels and falls as a vertical liquid stream. At the impingement point, the vertical slag stream has its minimal diameter and is subjected to strong shear forces which induce jet instability and breakup in the high-shear fiberization zone. Melt droplets (briefly connected by surface tension and viscous forces while nascent) are drawn out of the slag stream due to the propagation of microscopic instabilities on its external surface. The high-speed horizontal air jet transfers momentum to nascent fibers which follow parabolic trajectories while simultaneously undergoing cooling and elongation: as gravity prevails, cylindrical mineral wool fibers fly into a collection chamber and thus form a mineral wool layer. Off-spec product (spherical “shots”) either falls very close to the fiberization zone, or is trapped and inevitably solidified within the cooled material as it accumulates into the collection chamber.

The mathematical modeling strategy which is proposed in order to facilitate the study of molten slag fiberization is based on the concept of zone decomposition: as the process encompasses a variety of mass, heat and momentum transport phenomena, one can define 3 distinct zones, in each of which different phenomena prevail and different questions must be answered (Fig. 2b).

**Zone 1: Molten slag bulk flow.** The first zone of the fiberization process is the vertical slag stream emanating from the heated slag ladle: volumetric flow is controllable via ladle tilt angle. The prevalent phenomenon is macroscopic free surface laminar flow, also characterized by a nonisothermal temperature field (molten slag jet cooling due to forced convection and radiation). Both momentum and heat problems yield homogeneous solution fields with high observability.

**Zone 2: Mineral fiber generation.** The core zone of the fiberization process is the small volume within which the vertical slag stream disintegrates upon meeting the horizontal impinging air jet. The main phenomenon is microscopic molten slag fiber generation, characterized satisfactorily by the approximation of an isothermal temperature field, due to the very low residence times. The momentum problem yields an inhomogeneous two-phase field with rather low observability.

**Zone 3: Dispersed flow of fibers.** The final zone of the fiberization process is an extended cone produced by all isolated fiber trajectory curves emanating from the foregoing fiberization zone. This is a macroscopic dispersed flow zone, characterized by a nonisothermal temperature field with sharp gradients between and inside each fiber, due to their intensive cooling and elongation. The momentum problem yields a dynamic inhomogeneous field with moderate observability.



**Figure 2.** (a) Molten slag fiberization demonstration unit, (b) Mathematical modeling strategy and zone definition.

## Thermophysical Property Modeling and Operation Parameters

An extensive literature survey has led to numerous papers proposing elaborate thermophysical property models of silicate melts and validating most successfully against experimental data. Because molten slag properties (esp. density, viscosity and surface tension) are theoretically expected (and experientially known) to affect process operation (hence, product quality) to a significant extent, a computational investigation of property models is very important in order to: (a) a priori delineate property variation bounds for the given temperature range (1300-1800 °C), (b) comparatively validate the best of these models against pilot plant data as soon as possible, (c) calculate dimensionless numbers and their bounds and use them as plant diagnostic metrics, (d) correlate online property data with operation regimes during upcoming pilot plant campaigns.

**Density ( $\rho$ ).** The density correlation by Širok et al. (2008) has been employed to compute slag density values for representative compositions (Balomenos, 2010) in the 1300-1800 °C range. Density is determined to vary between  $2.589 \cdot 10^3 \text{ kg.m}^{-3}$  (1800 °C) and  $2.755 \cdot 10^3 \text{ kg.m}^{-3}$  (1300 °C).

**Viscosity ( $\mu$ ).** The viscosity correlation by Browning (2003) has been used so as to calculate slag viscosity values for the same representative compositions in the same 1300-1800 °C range. Viscosity is determined to vary greatly, between  $0.024 \text{ Pa.s}$  (1800 °C) and  $3.046 \text{ Pa.s}$  (1300 °C).

**Surface tension ( $\sigma$ ).** Due to the scarcity of temperature-dependent surface tension correlations, we decided to compile all surface tension measurements for adequately similar silicate slags. Based on a literature survey (Magidson et al., 2009; Arutyunyan et al., 2010) we have determined that slag surface tension varies between  $0.368 \text{ N.m}^{-1}$  and  $0.510 \text{ N.m}^{-1}$ , depending on composition.

**Operation parameters ( $d$ ,  $U$ ).** On the basis of video recordings of fiberization experiments, qualitative visual observations can be made about key dimensions and operation parameters. Slag jet diameter and velocity are estimated between  $0.05\text{-}0.20 \text{ m}$  and  $0.05\text{-}0.20 \text{ m.s}^{-1}$ , while slag drop diameter and velocity are estimated between  $0.001\text{-}0.01 \text{ m}$  and  $0.5\text{-}2.0 \text{ m.s}^{-1}$ , respectively.

Thermophysical properties as a function of temperature for fiberization are presented in Figure 3.

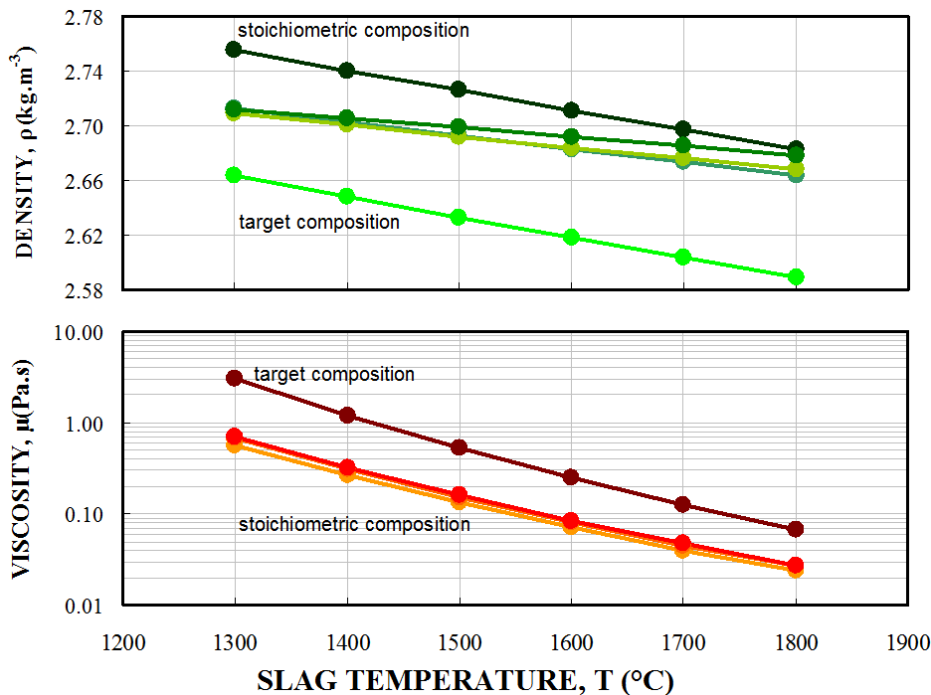


**Figure 3.** (a) Density, (b) Viscosity of molten red mud slags of variable composition as a function of temperature.

## Stochastic Fiber Generation and Flight Modeling

For a fundamental quantitative understanding of the mineral fiberization process within Zone 3, one must illustrate the dynamic mathematical model used to describe mineral fiber formation. Elaborate glass fiber cooling PDE models have been published and analyzed (Glicksman, 1968), while Nichiporenko et al. (1984) studied centrifugal melt jet atomization theoretically and experimentally, proving particle shape depends more on initial size than on cooling conditions. Detailed ODE models are published (Westerlund and Hoikka, 1989; Širok et al., 2008) for melt-spinning slag fiberization, but no study has hitherto focused on melt-blowing slag fiberization.

A number of fundamental simplifying assumptions are required in order to accurately capture the essential state variables of each slag fiber while ensuring compact model size and manageability. The fundamental assumption is that molten slag droplet cooling and fiber elongation occurs without significantly altering the external air flow field and without any secondary phenomena. Primary slag jet breakup occurs swiftly and entirely within very limited space and time (Zone 2). Air jet impingement on slag establishes a known, normal initial slag droplet velocity distribution as well as a known dispersion cone, whose apex is the initial position of all slag droplets at  $t = 0$ . Each spherical droplet remains an oblate ellipsoid which undergoes continuous transformation, with radius  $r(t)$ , length  $L(t)$  and temperature  $T(t)$  continuously varying under mass conservation. Mineral slag droplets and nascent fibers move unperturbed along independent flight trajectories and all secondary breakup, collision, coagulation and agglomeration phenomena can be ignored. The number and total mass of the entire molten slag particle population hence remains constant.

Each mineral slag particle has a uniform temperature (skin and internal gradients are negligible), which decreases continuously due to the combined effect of radiative and convective cooling. Radiative cooling induces fiber elongation, whose rate can be captured by an exponential model. Pressure gradients, slag capillary stress and external air flow field effects have been ignored here, and compositional variation effects within each droplet during its elongation are also negligible. Air thermophysical properties are constant, but molten slag ones are temperature-dependent. Controlled-rate molten slag melting and cooling experiments have been conducted at NTUA in order to determine the liquidus and solidus temperatures for red mud samples of ALSA, Greece. The liquidus temperature for red mud (first molten drop formation) is found:  $T_{liquidus} = 974$  °C. The solidus temperature for molten slag (first solid particle formation) is high:  $T_{solidus} = 1500$  °C. The initial slag droplet temperature (out of Zone 2) is thus taken here as:  $T_0 = 1000$  °C = 1273 K. Ambient air temperature is:  $T_{amb} = 300$  K, but within the flow:  $T_{air} = 600$  K (convective cooling).

Figure 4 summarizes the conceptual fiber evolution model as well as the underlying assumptions.

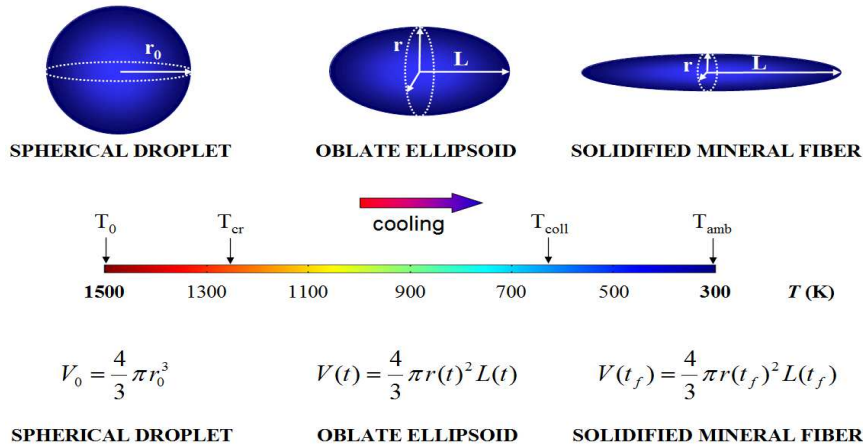


**Figure 4.** Conceptual mineral fiber elongation under continuous ellipsoidal transformation and mass conservation.

The mathematical model considers a fiber with mass  $m$ , diameter  $d$ , volume  $V$ , front surface  $A$ , heat capacity  $C_p$  and velocity  $v$  enters the air flow which has velocity  $v_{air}$  and temperature  $T_{air}$ . The forces exerted on the falling particle are the gravitational force ( $F_G$ ) which accelerates the mineral fiber, the buoyancy force ( $F_B$ ) and the drag force ( $F_D$ ) acting against the velocity vector:

$$\vec{F}_G = m\vec{g} \quad (1)$$

$$\vec{F}_B = \rho_{air} V\vec{g} \quad (2)$$

$$\vec{F}_D = \frac{1}{2} \rho_{air} C_D A (\vec{v}_{air} - \vec{v})^2 \quad (3)$$

The momentum balance on the flying mineral slag particle considers all forces exerted on it, and the mineral fiber velocity as a function of time is calculated by an ordinary differential equation:

$$\sum \vec{F} = m_p \frac{d\vec{v}}{dt} \Rightarrow \frac{d\vec{v}}{dt} = \frac{\rho_{slag} - \rho_{air}}{\rho_{slag}} \vec{g} - \frac{3}{4} \frac{\rho_{air} C_D (\vec{v}_{air} - \vec{v})^2}{\rho_{slag} d} \quad (4)$$

Therefore, the horizontal and vertical components of mineral fiber velocity are distinguished as:

$$\frac{dv_x}{dt} = -\frac{3}{4} \frac{\rho_{air} C_D (v_{air} - \sqrt{v_x^2 + v_y^2})^2}{\rho_{slag} d} \quad (5)$$

$$\frac{dv_y}{dt} = \frac{\rho_{slag} - \rho_{air}}{\rho_{slag}} g - \frac{3}{4} \frac{\rho_{air} C_D (v_{air} - \sqrt{v_x^2 + v_y^2})^2}{\rho_{slag} d} \quad (6)$$

The drag force coefficient ( $C_D$ ) is calculated using a Reynolds correlation by Glicksman (1968):

$$C_D = 0.4 \cdot Re^{-0.7} \quad (Re < 100) \quad (7)$$

Evidently, fiber flight trajectory coordinates are computed using velocity component definitions:

$$\frac{dx}{dt} = v_x \quad (8)$$

$$\frac{dy}{dt} = v_y \quad (9)$$

The mineral fiber length is considered to be a function of radiative cooling only and can thus be parameterized as an exponential function of a time-variant temperature differential ( $C_L = 0.02 \cdot r_0$ ):

$$\frac{dL}{dt} = C_L \exp(T - T_{amb}) \quad (10)$$

The complete mineral fiber heat balance is given by the following ordinary differential equation:

$$\frac{dT}{dt} = \frac{\alpha \cdot A(r, L)}{\rho_{slag} \cdot V(r, L) \cdot C_p} \cdot (T - T_{air}) + \frac{\varepsilon \cdot \sigma \cdot A(r, L)}{\rho_{slag} \cdot V(r, L) \cdot C_p} \cdot (T^4 - T_{amb}^4) \quad (11)$$

The heat transfer coefficient  $\alpha$  is given by a Nusselt correlation of Westerlund & Hoikka (1989):

$$Nu = 0.226 \cdot Re_d^{0.611} + 0.469 \quad (12)$$

Here,  $\varepsilon$  is the emissivity ( $\varepsilon = 0.85$ ), and  $\sigma$  is the Stefan-Boltzmann constant ( $5.6703 \text{ J} \cdot \text{m}^{-2} \cdot \text{s}^{-1} \cdot \text{K}^{-4}$ ).

## Stochastic Fiber Flight Simulation Results and Discussion

Melt-blowing slag fiberization is studied rigorously via an ODE system model in MATLAB<sup>®</sup>, considering unperturbed flight and simultaneous radiative cooling in a two-dimensional domain, assuming a normal initial slag droplet velocity distribution,  $\mathcal{N}(1, \sigma)v_{mean}$  (here,  $v_{mean} = 5 \text{ m}\cdot\text{s}^{-1}$ ). A sensitivity analysis of fiber flight trajectory swarms as a function of dispersion cone angle as well as velocity standard deviation shows great variability in flight length and deposition width. Figure 5 illustrates mineral fiber flight trajectory swarms for 200 identical droplets ( $r_0 = 5 \mu\text{m}$ ).

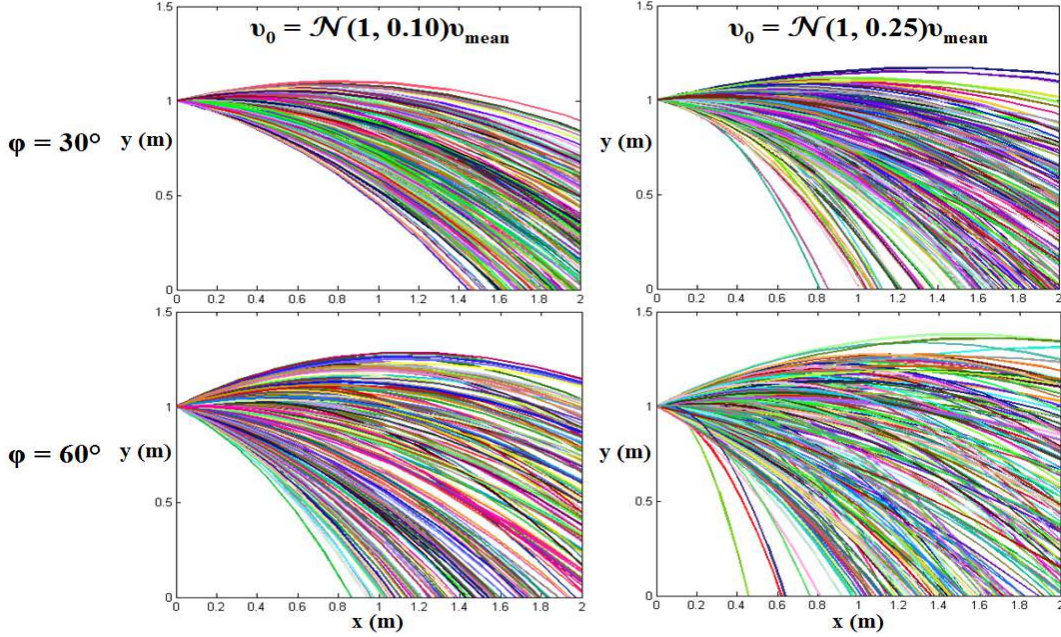


**Figure 5.** Mineral fiber xy-trajectories for different dispersion cone angles and initial velocity distributions ( $N=200$ ).

A sensitivity analysis of elongated fiber temperature and size as a function of initial droplet size has been performed in order to assess the importance of initial droplet size distribution (Zone 2). Figure 6 illustrates mineral fiber temperature and size evolution for various initial droplet sizes.

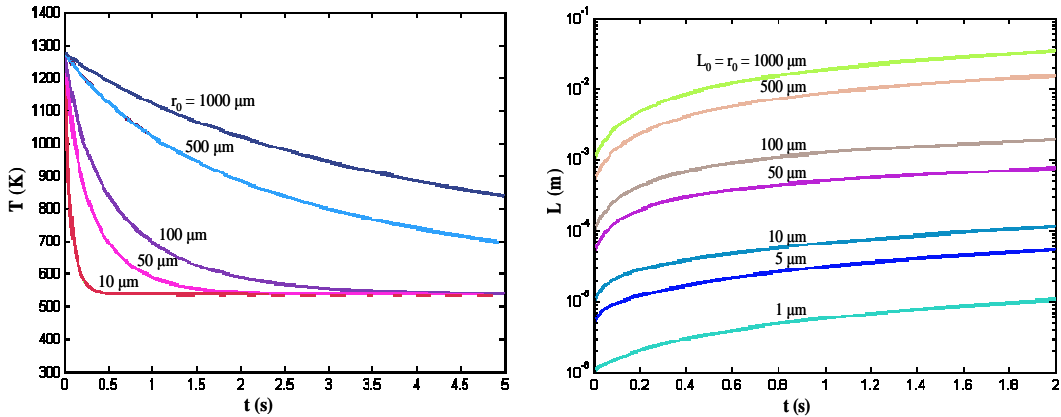


**Figure 6.** Mineral fiber temperature ( $T$ ) and elongation ( $L$ ) as a function of time for different initial particle sizes.

The fiber temperature evolution trend due to the combination of radiative and convective cooling corresponds very well to results obtained using a similar mathematical model (Širok et al., 2008). The fiber elongation plot indicates that high growth ratios (10-25) can be achieved in all cases.

## Conclusions

Molten inorganic slag fiberization has a strong industrial potential which requires detailed study: in particular, melt-blowing plants can surpass the widely established melt-spinning technologies. A mathematical modeling strategy for mineral slag fiberization has been outlined, on the basis of the concept that multiphase mass and heat flow can be studied efficiently in 3 distinct zones. Mathematical modeling is employed to study how fiber generation, flight and cooling dynamics under given process parameters affect fiber size distributions and thereby fiber size and quality. Thermophysical properties of slags (density, viscosity, surface tension) have been investigated in detail, and the best temperature-dependent correlations have been used to use reliable estimates. The nascent mineral fiber flight and elongation problem has been solved employing MATLAB<sup>®</sup>: fiber flight trajectory swarms as well as temperature and size evolution plots have been obtained. A sensitivity analysis of fiber flight trajectories indicates that elongated fiber scattering metrics increase for increasing dispersion cone angle and (even more) for increasing standard deviation, thereby implying that achieving a narrow, well-formed conical droplet spray in Zone 2 is critical in order to avoid unacceptably short or long trajectories and prevent extreme product variability. Flexibility in positioning the collection chamber is thus key towards minimizing material losses. A sensitivity analysis of fiber size and temperature with respect to initial droplet size confirms the importance of efficient slag atomization and is in excellent agreement with previous results.

## Acknowledgements

The authors gratefully acknowledge funding by the EU Seventh Framework Programme (FP7/2007-2013) under Grant Agreement No. ENER/FP7EN/249710/ENEXAL (Website: [www.labmet.ntua.gr/ENEXAL](http://www.labmet.ntua.gr/ENEXAL)).

## References

1. AMRT-Advanced Mineral Recovery Technologies, <http://amrt.co.uk/index.html> (2011).
2. Arutyunyan, N.A., Zaitsev, A.I., Shaposhnikov, N.G., Surface tension of CaO-Al<sub>2</sub>O<sub>3</sub>, CaO-SiO<sub>2</sub> and CaO-Al<sub>2</sub>O<sub>3</sub>-SiO<sub>2</sub> melts, *Rus. J. Phys. Chem. A* **84**(1): 7-12 (2010).
3. Balomenos, E., *Thermodynamic study of red mud treatment*. ENEXAL Technical Report, NTUA (2010).
4. Browning, G.J., Bryant, G.W., Hurst, H.J., Lucas, J.A., Wall, T.F., An empirical method for the prediction of coal ash slag viscosity, *Energy & Fuels* **17**(3): 731-737 (2003).
5. Frank W.B. et al., *Aluminium*, Wiley-VCH Verlag GmbH & Co (2005).
6. Gerogiorgis, D.I., *Multiscale Process and CFD Modeling for Distributed Chemical Process Systems: Application to Carbothermic Aluminium Production*, PhD Thesis, Carnegie Mellon University (2004).
7. Glicksman, L.R., The cooling of glass fibers, *Glass Technol.* **9**(5): 131-138 (1968).
8. Haupin, W., Aluminum production and refining, in: Buschow K.H. et al. (editors), *Encyclopedia of Materials: Science and Technology*, pp. 132-141, Elsevier, Amsterdam (2001).
9. Kumar S. et al., Innovative methodologies for the utilisation of wastes from metallurgical and allied industries Resources, *Conserv. Recycling* **48**: 301-314 (2006).
10. Magidson, I.A., Basov, A.V., Smirnov, N.A., Surface tension of CaO-Al<sub>2</sub>O<sub>3</sub>-SiO<sub>2</sub> oxide melts, *Rus. Metal. (Metally)* **2009**(7): 631-635 (2009).
11. Maitra P.K., Recovery of TiO<sub>2</sub> from red mud for abatement of pollution and for conservation of land and mineral resources, *Light Metals*, pp.159-165 (1994).
12. Nichiporenko, O.S., Tsipunov, A.G., Ternovoi, Y.F., Analysis of the particle shape formation process in the centrifugal atomization of a melt jet, *Powder Metall. Met. C.* **23**(1): 1-6 (1984).
13. Santana L., Castaldi P., Melis P., Evaluation of the interaction mechanisms between red muds and heavy metals, *J. Haz. Mat.* **136**: 324-329 (2006).
14. Širok, B., Blagojevic, B., Pullen, P., *Mineral Wool – Production and Properties*, Woodhead Publishing (2008).
15. Wang S. et al., Novel applications of red mud as coagulant, adsorbent and catalyst for environmentally benign processes, *Chemosphere* **72**: 1621-1635 (2008).
16. Westerlund, T., Hoikka, T., On the modeling of mineral fiber formation, *Comput. Chem. Eng.* **13**(10): 1153-1163 (1989).